6th Congress of Alps-Adria
Acoustics Assosiation
16.-17. October 2014
Graz, Austria

Austrian Acoustics Association
Österreichische Gesellschaft für Akustik

Alps Adria Acoustics Association

ISBN: 978-3-200-03921-6

SENSOR FOR IN-SITU MEASUREMENTS OF SOUND ABSORPTION

Jurij Prezelj, Primož Lipar, Peter Šteblaj, Mirko Čudina

University of Ljubljana, Faculty of mechanical engineering, prezelj.jurij@gmail.com

Abstract: *A theoretical background and some measurement results for a new technique intended for in-situ measuring of sound absorption are presented. The measurement technique is a refinement of the classical method using reflection over the impedance plane. Refinement is based on the directivity pattern of dipole source in a very near field. Presented measurement results of absorption are obtained with basic evaluation of noise spectra. Comparison between measured absorption and absorption from kundt tube, are in good agreement, except in frequency range where absorption significantly depends on the flow resistivity of measured sample. Therefore a theoretical analysis was performed to found the source for this mismatch. Theoretical analysis of acoustical setup is based on the Rayleigh integral, which is used for calculations of sound propagation from complex sources, with integrated Delany-Bazly-Miki model. Analytical results with numerical simulations based on FEM analysis are compared in this preliminary study. Results of theoretical analysis indicate that calculation of absorption in low frequency range should be based on flow resistivity, whereas in higher frequency range a simple evaluation of noise spectra is sufficient. Theoretical results provide an excellent starting point for the design platform of the new sensor for sound absorption.*

Key words: Flow resistivity, Sound absorption, Sound reflection, Very Near Field

1. INTRODUCTION

Reflection and absorption of sound from an impedance plane is important topic in many engineering examples. During the design stage of different acoustic projects a knowledge of expected absorption is necessary. Many different materials are available and information about their acoustic properties is provided by their producers. Quality of such materials is often overestimated. Different materials can be merged together with different structures and forming number of different and unique acoustic elements with unknown acoustic properties. Properties of different elements also deteriorate with time. Measurements of sound absorption/reflection are therefore necessary and therefore a common practice in acoustical engineering. Measurements of sound absorption on-site are particularly interesting. Numerous ways of measuring the reflection or absorption coefficient in-situ were developed. Such measurements in industrial environment are quite difficult to perform, partially because of the reverberant conditions, and partially because of the background noise, [1, and 2]. In available literature no methods were found describing the in-situ measurement of sound absorption in very low frequency range, below 100 Hz. Development of methods is primarily oriented towards digital signal processing and only few attempts were made to improve methods in the acoustic domain. However, even the most sophisticated DSP algorithms cannot compensate for poor acoustic design.

A microphone doublet method was designed more than 20 years ago. It is simple and accurately working at low frequencies, but it needs to have a sound source mounted at a sufficient distance, to generate approximately plane waves near the sample, which is a strong limitation for routine on-site measurements in noisy environment, [3, 4]. The use of the Microflown PU sensor seems to be efficient for measuring sound absorption in frequency range above 200 Hz and up to 3 kHz, [5, 6].

A use of powerful ultrasonic demodulated waves in air has proved to be a very attractive tool to characterize the audio range acoustical properties of absorbing porous materials, which are described with the background of the equivalent fluid rigid frame. The very unique feature of that technique, mainly due to its high directivity producing plane waves, lies on the fact that it can work in air in the free field, allowing simple and straightforward in situ measurements, at least if a proper procedure is used. Such method can be used in frequency range from 100 Hz up to 4 kHz, [7].

A lot of applications for in-situ measurement of sound absorption use what may be called a reflection or impulse echo method which analyses an impulse shaped signal reflected from the surface under consideration. Methods which are based on the measurement of reflection usually use different shapes of pulses. Different digital signal processing algorithms are then used to separate the reflected wave from the incidence wave in time domain. This separation process is needed because the microphone is usually placed close to the measuring surface to achieve sufficient signal to noise ratio of the reflected wave. By using such an approach and by subtraction method, useful results can be expected in frequency range from 250 Hz to 8 kHz, if a sample is large enough, at least 4 m2, [8, 9].

Some attempts were made to focus the sound beam in order to minimize the needed surface area for testing by using an array of microphones. Such measurement of the sound absorption coefficient of flat panels subject to small angle sound incidence, in an industrial hall using an experimental device equipped with an acoustic array are expected to work in frequency range from 250 Hz to 4 kHz, [1].

Kimura developed a system based on a stretched pulse. Such a system consists from more loudspeakers and one moving loudspeaker. This method provides useful results of sound absorption determination and the directivity of sound absorption in frequency range from 400 Hz up to 4 kHz, [10].

None of known methods satisfies all demands: Lightweight measurement equipment, broad frequency range, simplicity, fast results, and comparable results with laboratory standardized results. Therefore a new approach of using so-called Very Near Field (VNF) around the dipole source was investigated. Numerical results are presented and they indicate that sound pressure in the VNF around dipole sound source, placed close to the porous surface, strongly depends on the flow resistivity of the surface.

2. DIPOLE SOURCE ABOVE THE IMPEDANCE PLANE

Sketch of the experiment is presented in Fig.1. Measurement of sound pressure or sound intensity in the VNF of the dipole can be correlated to the acoustic properties of this porous surface, [11, 12, 13, 14, 15, 16].

Many papers deal with absorption of a spherical wave by an absorbing plane. In particular, prediction of the sound field due to a simple point source in a homogenous medium above an impedance plane is a fundamentally important problem in many applications of outdoor acoustics and noise control engineering, which has been pursued by many authors. However, only few authors discussed problem of dipole source over impedance plane [11, 12, 13, 14].

Hess, et al. studied the influence of ground reflection coefficient on the sound pressure field, for the purpose of ground impedance evaluation using dipole with similar measurement setup as depicted in Fig.1, however they were performing all measurements in a far field of the dipole source. They found out that the logarithm of the ratio of total field to the direct field (a spectrum of the excess attenuation), contains a characteristic series of minima and maxima. Amplitude value of the first maximum or minimum in excess attenuation spectrum is very sensitive to ground impedance, [16]. Frequency of the peaks and deeps depends on the geometry of the setup. Ratio between the height of the dipole above impedance plane (H), and position of the observation point is important, [16]

Allard et al. discussed indoor measurement of ground impedance at low frequencies, as well as in an anechoic room on similar setup. One of their conclusions was that the dipole source and the microphone must be placed close to each other, in order to increase the contribution of the direct field, [17].

K.M.Li, et.al, followed to Allard's conclusions and developed analytical solutions for sound propagation from dipole source and quadruple source near an impedance plane [12, 13]. Their solution is general and includes different orientations of the dipole source for arbitrary location of the receiver. Numerical results of excess attenuation spectra are given for different theoretical setups, as well as for SPL as function of distance from the source. Presented results of vertical dipole source placed a few cm above the impedance plane indicate that in frequency range below 100 Hz exist a possibility to measure excess attenuation to obtain surface impedance.

Hasheminejad et al. discussed theoretical dipole and sound pressure in a Very Near Field (kr=0.05), [11]. However they didn't consider the results to be limited by practical dimensions of the dipole sources. If kr<0.1 then dimensions of the dipole are already important for the behavior of the sound field in higher frequency range. Therefore another approach by using Rayleigh integral for calculation of sound in a Very Near Field of the plate is needed, as described in [17].

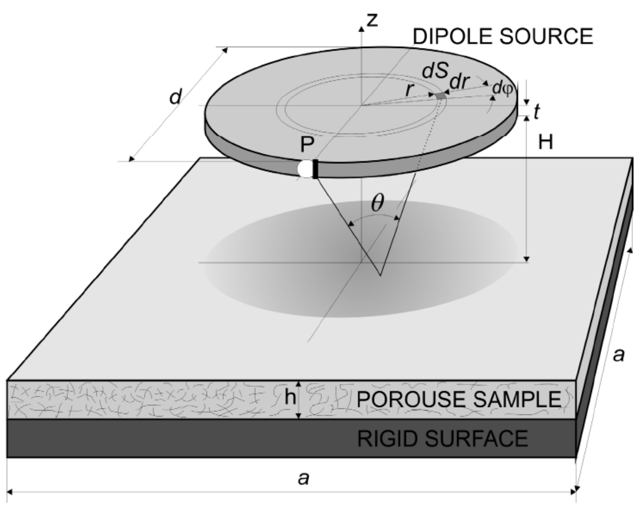

Fig. 1. Geometry of the theoretical setup

3. EXPERIMENTAL SETUP

In order to satisfy conditions for sufficient response in low frequency range and geometrical conditions of narrow acoustic short circuit area in high frequency range, two sensors were developed; one for low frequency range and other for higher frequency range.

3.1 Low frequency range

To obtain sufficient signal to noise ratio in the low frequency range more loudspeaker were mounted together in a configuration shown in Fig. 2.

Fig. 2. A dipole configuration used for low frequency range

Loudspeakers with a diameter of 10 cm were used. They have a linear excursion of +/- 3 mm and maximum excursion of +/- 4 mm. additionally, two loudspeakers were put together in a push-pull configuration to obtain pure dipole source. Two pairs of loudspeakers were mounted together side by side, in order to increase the signal to noise ratio. Microphone was placed between the two pairs, in the center area of the acoustic short circuit.
Results of sensor frequency response to pink noise are given in Fig. 3, for three different acoustic environments;

- free field,
- sensor placed over the reflecting surface and
- sensor placed over the sample on the reflecting surface as depicted in Fig.1.

Blue spectrum in Fig. 3 presents a sound pressure on the microphone, when the sensor was placed in a free field. Red spectrum in Fig. 3 presents a sound pressure on the microphone, when the sensor was placed over the reflecting surface. Green spectrum presents a sound pressure on the microphone, when the sensor was placed over the sample on the reflecting surface.
Signal to noise ratio is over 10 dB at 50 Hz and more than 25 dB at 300 Hz. If the sensor is placed over the sound absorbing sample, than the values of sound pressure in low frequency range below 100 Hz are practically the same as if it would be placed on the reflecting surface without the sample. This is according to the theory as sound absorption in low frequency range is for thin porous sample close to 0. The values of sound pressure in high frequency range above 1600 Hz are closer to the values as the sensor would be placed in the free field. This is according to the theory as sound absorption in high frequency range is close to 1 for porous sample.
However, due to the presence of acoustic minima and maxima in the sound pressure at the microphone location in the very near field of the sensor, the upper limit of the frequency range is just around 1600 Hz. Above 1800 Hz the value of sound pressure spectrum measured over the sample is lower from the sound pressure spectrum measured in a free field. This would indicate to the sound absorption coefficient higher then 1, which is impossible. Therefore a need for additional sensor appears which would be more suited for measurements high frequency range.

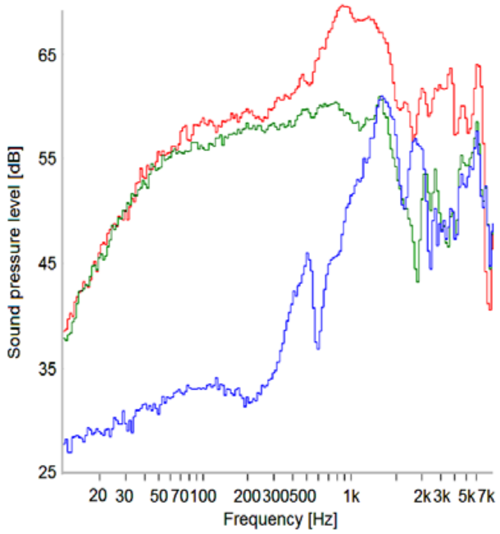

Fig. 3. Results of measurements with a configuration used for low frequency range

3.2 High Frequency range

Additional dipole was constructed with smaller loudspeakers, Fig. 4. Results of sensor frequency response to pink noise are given in Fig. 5. Usable frequency range has shifted towards higher frequency range, up to 4000 Hz. However, the response in low frequency range below 200 Hz is now unusable.

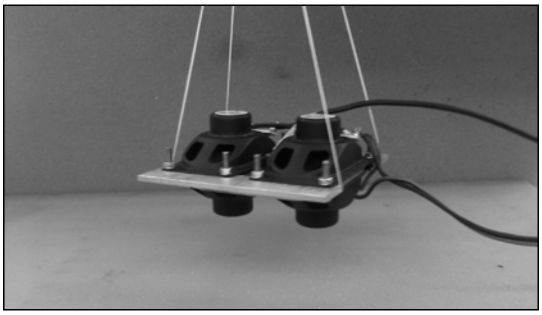

Fig. 4. A dipole used for high frequency range

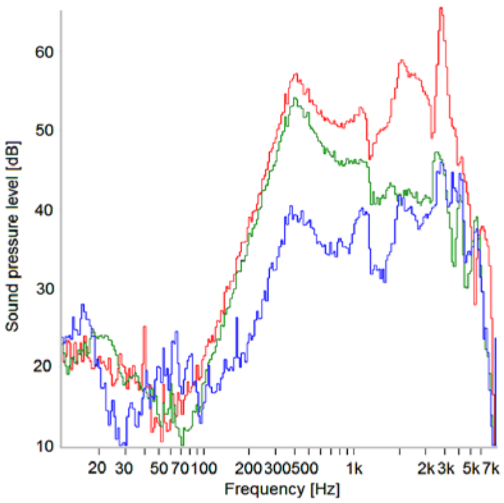

Fig. 5. Results of measurements with a quadruple configuration used for low frequency range

4. RESULTS OF MEASUREMENTS THE SOUND ABSORPTION COEFFICIENT

Assessment of sound absorption from three measured spectra can be performed according to Eq.1.

$$\alpha(f) = 1 - \frac{P_{r,a}(f) - P_{r,s}(f)}{P_{r,a}(f) - P_{r,b}(f)} \qquad (1)$$

Where $P_{r,a}$ stands for noise spectra above reflecting plane, $P_{r,s}$ stands for noise spectra above sample plane and $P_{r,b}$ stands for noise spectra of sensor in free field. Measurement results for acoustic foam with density of 50 kg/m^3 and thickness of 50 mm are presented in Fig. 6. Green spectrum of sound absorption coefficient is measured with smaller sensor presented in Fig.4. Blue spectrum is measured with larger sensor presented in Fig.2. We can see that smaller sensor does not provide logical results in frequency range below 120 Hz. On the other hand larger sensor provides very satisfying results from the lowest frequencies and up to 1600 Hz. Results of larger sensor in frequency range above 1600 do not coincide with anticipated results. Smaller sensor provides results up to 4 kHz.

In order to cover the whole frequency range of interest, results obtained with two differently sized sensors were merged together accordingly to their frequency range. Values were weighted according to appropriate frequency range as given in Eq. 2. Furthermore, value at the discrete frequency f_j is calculated as an averaged value of three values around this selected frequency.

$$\alpha(f_j) = \frac{1}{3}\sum_{i=1}^{3} K_{LF}(f_{j-1+i})\alpha_{LF}(f_{j-1+i}) + K_{HF}(f_{j-1+i})\alpha_{HF}(f_{j-1+i}) \qquad (2)$$

K_{LF} and K_{HF} are weighting coefficients which depend on the frequency, (Fig 7). Their sum is 1. α_{LF} is measured sound absorption with the larger sensor and α_{HF} is measured sound absorption with a smaller sensor. Combined result is presented in Fig. 6 as the red spectrum of sound absorption.

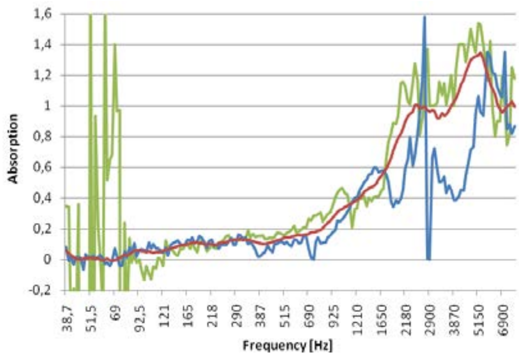

Fig. 6. Results of sound absorption coefficient

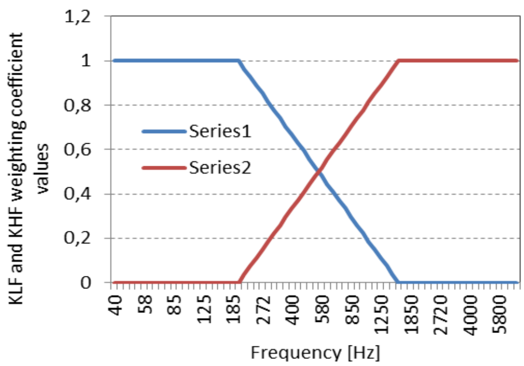

Fig.19. Weighting coefficients, K_{LF} blue curve and K_{HF} red curve

After the measurement procedure was in operation, additional measurements were performed on different sample made from different type of polyurethane foam with different density and with different structure.
Measured spectra of sound absorption coefficient were compared with values obtained in impedance tube with SWR method. Comparison is presented in Fig. 8 for two different samples. Results of measurements with impedance tube are given in frequency range from 100 Hz to 4 kHz. Results of measurements with our method are given in frequency range from 31,5 Hz to 4000 Hz. A correlation is obvious. However two methods have provided different results in frequency range below 1000 Hz. In order to establish why differences occur, a theoretical analysis was performed with the emphases on the analysis of the influence of the flow resistivity on the measured absorption.

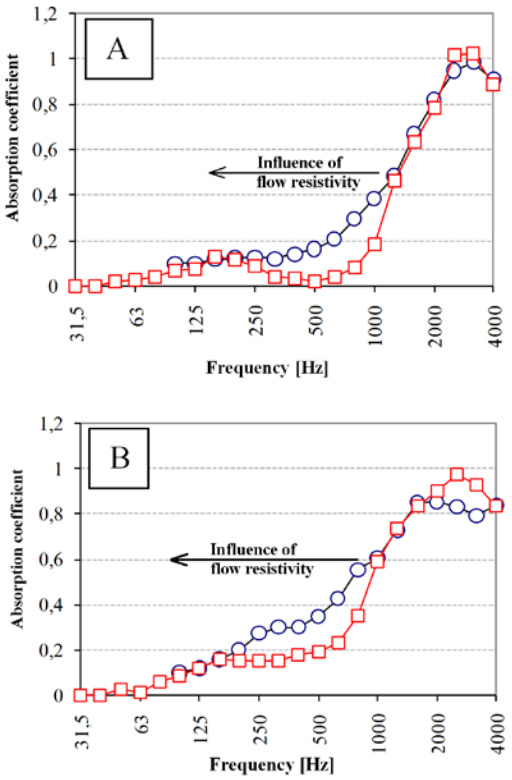

Fig. 8. Comparison of results; sound absorption coefficient measured in an impedance tube – blue curve, coefficient measured with a dipole in a Very Near Field – blue curve. A: polyurethane foam, 10 mm thick, with density 60kg/m3, B: Polyurethane foam, 40 mm thick with density 50kg/m3

5. INFLUENCE OF FLOW RESISTIVITY

Influence of flow resistivity was analytically and numerically analyzed by introducing the Delany-Bazely-Miki model of sound absorption into the Rayleigh surface integral. Rayleigh surface integral was used for the calculation of generated sound pressure on the vibrating surface.

Let us consider an arbitrary vibrating surface ***V*** in an acoustic free field. A complex vibrating surface can be divided on many elementary surfaces d*S*. Each elementary surface d*S* on the arbitrary shaped surface can be regarded as a simple point source of an outgoing sound wave, if the wavelength of the generated sound is much longer than the dimensions of this elementary source d*S*. In order to avoid pressure build up between the dipole source and sample, the minimum height of the dipole was $H_{min}=d/4$. Sound pressure, radiated from an arbitrary shaped surface can be calculated at the arbitrary location *P* by using the Rayleigh surface integral given in Eq.(3), where ω stands for the frequency, ρ_0 for density of the air, *k* is wave number and *v* is the vibration velocity of the elementary source d*S*. A discretization of the vibrating surface is presented in Fig. 1.

$$p(x_0, y_0, z_0) = \frac{i\omega\rho_0}{2\pi}\iint_S \Re(\theta)\frac{e^{-ikR}}{R}v(x,y)dS \quad (3)$$

A complex reflection coefficient in Eq.(3) is denoted with $\Re(\theta)=\alpha+\beta i$. This reflection coefficient depends on the incidence angle θ, which can be easily correlated with the path *R* from the partial source d*S* to the selected imission point *p*:

$$R=\sqrt{4H^2+r^2+\frac{d^2}{4}-rd\cos\varphi} \quad (4)$$

$$\cos\theta=\frac{2H}{R} \quad \text{and} \quad \sin\theta=\frac{\sqrt{r^2+\frac{d^2}{4}-rd\cos\varphi}}{R} \quad (5)$$

Snell's law for reflection coefficient can be expressed as:

$$\Re(\theta)=\frac{Zs\sin\theta-\dfrac{Z_0}{\cos\theta}}{Zs\sin\theta+\dfrac{Z_0}{\cos\theta}} \quad (6)$$

Where *Zs* is surface impedance of the sample and Z_0 is characteristic impedance of air. Surface impedance of the sample was estimated by Delany - Bazley - Miki (DBM) AbsoMethod, [18]. Surface impedance of the locally reacting absorber can be evaluated from the flow resistivity of the sample, denoted with σ in Eq.(7), according to the DBM method, [7]:

$$Z_s=\rho_0 c_0\left[1+5{,}5\left(1000\frac{\omega}{2\pi\sigma}\right)^{-0{,}632}-8{,}43i\left(1000\frac{\omega}{2\pi\sigma}\right)^{-0{,}632}\right] \quad (7)$$

If we apply cylindrical system into Eq.(3), we can write the solution for the sound pressure at the edge of the vibrating surface at *r=d/2*. Vibrating surface can be regarded as un-baffled piston if $kd<\pi$. Sound pressure wave from the positive side of the elementary dipole d*S* is always superimposed by its negative wave at the observation point. Only the reflected sound pressure wave contributes to the acoustic pressure at the observation point. If only the reflected wave is included into the calculations of Eq.(3) and if it is rewritten into the cylindrical coordinates, Eq.(8) is obtained. Integral in Eq.(8) is expressed with all known variables, and it can be easily numerically solved. Values under the Square-root in the denominator of the surface integral are always positive, therefore solution is simple and it can be easily transferred into discrete numerical calculation.

$$p = \frac{ik\rho_0 c_0}{2\pi} v_0 \int_{r=0}^{d/2} \int_{\varphi=0}^{2\pi} \frac{Zs\sin\theta - \frac{Z_0}{\cos\theta}}{Zs\sin\theta + \frac{Z_0}{\cos\theta}} *$$

$$* \frac{e^{-ik\sqrt{r^2+\frac{d^2}{4}-dr\cos\varphi+4H^2}}}{\sqrt{r^2+\frac{d^2}{4}-dr\cos\varphi+4H^2}} r d\varphi dr \qquad (8)$$

Results for a thin circular piston of 200 mm in diameter and placed 50 mm above the reflecting impedance plane are presented in Fig.9. Black thick curve presents a sound pressure spectrum at the observation point *p* if the dipole is placed above the perfectly reflecting plane with $\Re(\vartheta) = 1$. Value for flow resistivity of reflecting plane was set to 10^9 kPa s/m^2. Grey curves presents a sound pressure spectrum of at the observation point if the dipole is placed over the impedance plane with different reflections, calculated accordingly from different values for flow resistivity. Values ranged from 3, 10, 33, 100, 333, 1000, 3333, 10000, 33333 to 100000 kPa s/m^2. The lowest value represents the impedance match, where no reflection should occur and no sound pressure level should be established at the observation point. The highest value represents a reflection from a rigid surface. Reflection from the rigid surface generates highest sound pressure spectrum.

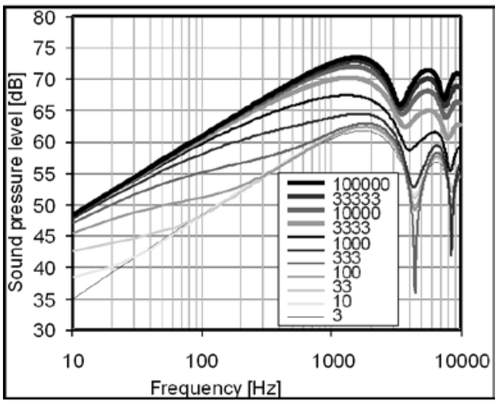

Fig. 9. Numerical results for sound pressure at the observation point

The most important result of the theoretical setup is that spectrum values differ for 13 dB in broad frequency range, up to 1650 Hz. At this frequency, the dipole dimensions equals wavelength of the generated sound. A 13 dB difference is sufficient to solve the inverse problem. A sound reflection coefficient can be estimated, by comparing a sound pressure above different but well defined impedance planes, to a sound pressure above the unknown sample.

6. FEM ANALYSIS

A numerical analysis was performed using a Finite Element Method (FEM). FEM analysis exploited axial symmetry of the setup for proper 3 dimensional simulation of wave propagation from un-baffled vibrating circular rigid plate. Linear elastic fluid model was used for surrounding air and Delany-Bazley fluid model was used to simulate sample as a locally reacting absorber. Setup of the numerical simulation is presented in Fig. 10.

Numerical experiments were performed to determine the correlation between the sound pressure, around the dipole, and acoustical properties of the sample. Results are presented in Fig. 11. In frequency range above 1000 Hz Spectra differs in levels and frequencies of minima and maxima, which cannot be easily interpreted. However, a lucid influence of flow resistivity can be observed in frequency range below 1000 Hz. Spectrum values are shifting towards higher values with higher flow resistivity. Such result is expected, because intuitively we know that hard surface reflects sound more efficiently and higher values of sound pressure are expected.

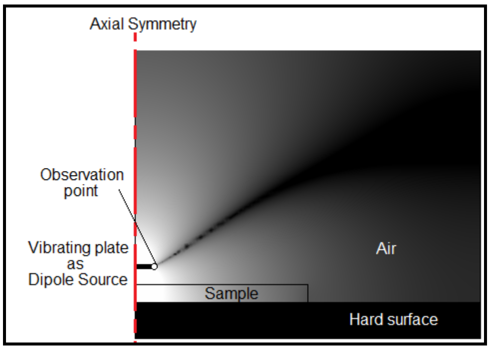

Fig.10. FEM model

In order to correlate the flow resistivity with the sound pressure levels, a correlation was observed at three different frequencies; 10 Hz, 50 Hz and 300 Hz. Results are presented in Fig. 12. Curves represent theoretical results using Rayleigh integral and markers represent results obtained with FEM analysis. Influence of flow resistivity on the sound pressure level is frequency dependent. Subsonic frequency sound at 10 Hz is already affected by a sample with flow resistivity around 10 kPa s/m^2. Sound pressure level at 250 Hz is affected by a sample with higher flow resistivity, around 333 kPa s/m^2. Flow resistivity can be therefore determined from measurements of sound pressure level in frequency range below 1000 Hz.

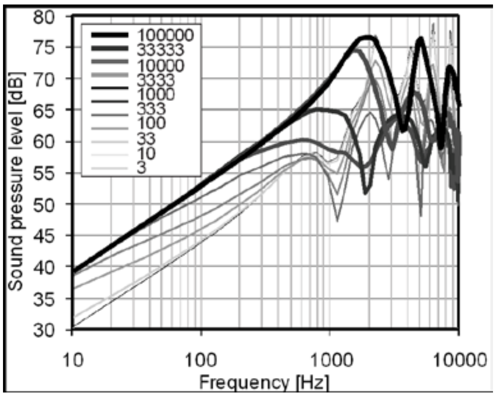

Fig.11.Sound pressure at point *p* obtained with FEM analysis

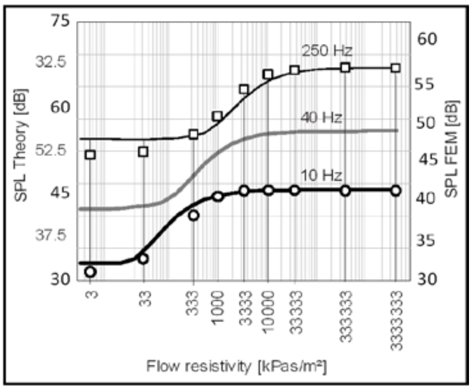

Fig.12. Correlation between sound pressure level at the observation point and flow resistivity of the sample

5. CONCLUSIONS

Experimental results proved that the described principle of sound absorption measurement is working. Correlation between results of sound absorption, measured with dipole source in a Very Near Field, and sound absorption, measured in the Kundt tube, show encouraging results. However, results indicate that in low frequency range, below 1000 Hz, method actually measures the flow resistivity of the sample, and that in the calculation of sound absorption flow resistivity needs to be incorporated.

Results of numerical calculations, based on Rayleigh integral, shoved that the dipole source, in the form of a vibrating plate can be placed close to the impedance plane. Sound pressure in the Very Near Field of the dipole strongly depends on the properties of the impedance plane. Theoretical calculations based on Rayleigh integral with incorporated Delany-Bazely-Micki model for impedance, and with Snell's law, showed, that sound pressure level in the ring of the dipole strongly depends on the flow resistivity of the impedance plane.

Results of FEM simulations confirmed that sound pressure in the ring of a dipole source, where acoustic short circuit occurs, depends on the acoustic properties of the surface near dipole source. Sound pressure in the node of a dipole depends on the acoustic properties of the surface in the very near field of a dipole source.

Theoretical results provide an excellent starting point for the design platform of the new sensor for sound absorption. In further work a theoretical correlation between sound pressure in the ring of the dipole source, flow resistivity and sound absorption will be improved by adding by radiation impedance of the dipole source.

6. REFERENCES

[1] E. Mommertz, Angle - Dependent In - Situ Measurements of Reflection Coefficient Using a Subtraction Method, *Applied Acoustics*, vol. 46, 1995, pp. 251-263

[2] J. Ducourneau, V. Planeau, J. Chatillon, Nejade, Measurement of sound absorption coefficients of flat surfaces in a workshop, *Applied Acoustics*, vol. 70 (2009), pp. 710–721

[3] E. Tijs, E. Druyvesteyn, An Intensity Method for Measuring Absorption Properties in situ, Acta *Acustica united with Acustica*, vol. 98 (2), 2012 , pp. 342-353

[4] Y. Takahashi, T. Otsuru, R. Tomiku, In situ measurements of surface impedance and absorption coefficients of porous materials using two microphones and ambient noise, *Applied Acoustics*, vol. 66, 2005 pp. 845–865

[5] R. Lanoye, G. Vermeir, W. Lauriks, Measuring the free field acoustic impedance and absorption coefficient of sound absorbing materials with a combined particle velocity-pressure sensor, *J. Acoust. Soc. Am*, vol.119 (5), 2006, pp 2826-2831

[6] M. Muller, P. Dietrich, M. Aretz, J. Gemmeren, and M. Vorlander, On the in situ impedance measurement with pu-probes— Simulation of the measurement setup, *J. Acoust. Soc. Am.* vol 134 (2), 2013, pp.1062-1089

[7] B. Castagne´de, A. Moussatov, D. Lafarge, M. Saeid, Low frequency in situ metrology of absorption and dispersion of sound absorbing porous materials based on high power ultrasonic non-linearly demodulated waves, *Applied Acoustics*, vol. 69, 2008, pp. 634–648

[8] C. Nocke, In-situ acoustic impedance measurement using a free-field transfer function method, *Applied Acoustics* vol. 59, 2000, pp. 253-264

[9] P.A. Morgan, G.R. Watts,A novel approach to the acoustic characterization of porous road surfaces, *Applied Acoustics*, vol. 64 2003, pp. 1171–1186

[10] K. Kimura, K. Yamamoto, A method for measuring oblique incidence absorption coefficient of absorptive panels by stretched pulse technique, *Applied Acoustics*, vol.62, 2001, pp. 617-632

[11] S.M. Hasheminejad, M. Azarpeyvand, Modal vibrations of a cylindrical radiator over an impedance plane, *Journal of Sound and Vibration*, vol. 278, pp. 461–477, 2004

[12] K. M. Li, S. Taherzadeh, K. Attenborough, Sound propagation from a dipole source near an impedance plane, *Journal of Acoustical Society of America*., 101(6), pp 3343-3352, June 1997

[13] K. M. Li, S. Taherzadeh, The sound field of an arbitrarily oriented quadrupole near ground surfaces, *Journal of Acoustical Society of America*, 102(4), pp 2050-2057, October 1997

[14] K. M. Li, H. Tao, Reflection and Transmission of Sound From a Dipole Source Near a Rigid Porous Medium, *Acta Acustica united with Acustica*, vol. 99, 2013, pp. 703 – 715

[15] H.M. Hess, K. Attenborough, N.W. Heap, Ground characterization by short-range propagation measurements, *Journal of Acoustical Society of America*, vol.87(5), pp.1975-1986, May 1990

[16] J.F. Allard, Y. Champoux, J. Nicolas, Pressure variation above a layer of absorbing material and impedance measurement at oblique incidence and low frequencies, *Journal of Acoustical Society of America*, vol.86(2), pp.766-770, August 1989

[17] J. Prezelj, P. Lipar, A. Belsak, M.Čudina, On acoustic very near field measurements, Mechanical systems and signal processing, vol.40, pp.194-207, June 2013

[18] Y.Miki, Acoustical properties of porus materials - modification of D-B model, *J.Acoust.Soc.Jpn*, vol.11(1), 1990, pp. 19-24